

## Antiferroelectric Liquid Crystal from Bent-Core Molecule with Vinyl End Group

Chong-Kwang Lee,<sup>\*</sup> Soon-Sik Kwon, Tae-Sung Kim, Sung-Tae Shin,<sup>†</sup> Hong Choi,<sup>†</sup>  
E-Joon Choi,<sup>‡</sup> Sea-Yun Kim,<sup>‡</sup> Wang-Choel Zin,<sup>§</sup> Dae-Choel Kim,<sup>§</sup> and Liang-Chy Chien<sup>#</sup>

*Dept. of Chemistry, Gyeongsang National University, Jinju 660-701, Korea*

*<sup>†</sup>Dept. of Physics, Korea University, Chungnam 339-700, Korea*

*<sup>‡</sup>Dept. of Polymer Science and Engineering, Kumoh National University of Technology, Kumi 730-701, Korea*

*<sup>§</sup>Dept. of Material Science and Engineering, Pohang University of Science and Technology, Pohang 790-784, Korea*

*<sup>#</sup>Liquid Crystal Institute, Kent State University, Kent, Ohio 44242, USA*

*Received April 1, 2004*

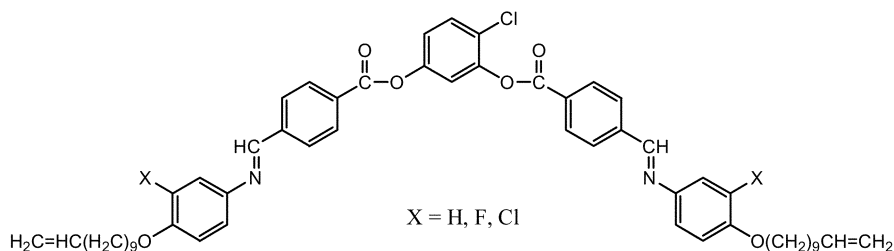
Three banana-shaped achiral compounds, 4-chloro-1,3-phenylene bis [4-{4-(undecenyloxy)phenyl imino-methyl}benzoate] derivatives, were synthesized with variation of a substituent ( $x=H, F, Cl$ ); their antiferroelectric properties are described. The smectic mesophases, including a switchable chiral smectic  $C(Sm C^*)$  phase, were characterized by differential scanning calorimetry, polarizing optical microscopy, triangular wave method, and X-ray diffractometry. The presence of vinyl groups at the terminals of linear side wings in the banana-shaped achiral molecules induced a decrease in melting temperature and formation of the switchable  $Sm C^*$  phase in the melt. The smectic phase having a lateral fluorine-substituent at 3-position of the Schiff's base moiety showed antiferroelectric switching, and the value of spontaneous polarization on reversal of an applied electric field was  $250 \text{ nC/cm}^2$ .

**Key Words :** Banana-shaped liquid crystal, Switchable smectic C, Spontaneous polarization, Antiferroelectric properties, Bent-core molecule

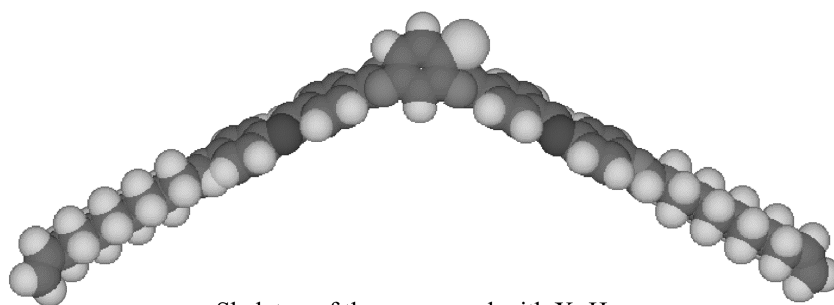
### Introduction

Most chirality of liquid crystal phases can be obtained by the introduction of a group containing a chiral carbon. The chiral mesophase without the chiral structure can also occur by spontaneous polarization derived from symmetry break-

ing.<sup>1-3</sup> Ferroelectric liquids (FLCs) due to the spontaneous polarization are now regarded as one of the most promising property of optoelectronic materials.<sup>4,5</sup> A fascinating example of the achiral symmetry breaking was found in the tilted smectic phases of banana-shaped molecules.<sup>6,7</sup> Because of the director tilt and the simultaneous polar ordering, each



4-chloro-1,3-phenylene bis [4-{4-(10-undecenyloxy)phenyliminomethyl}benzoate]



Skeleton of the compound with  $X=H$

<sup>\*</sup>Author for correspondence. e-mail: cklee@nongae.gsnu.ac.kr

smectic layer loses its inversion symmetry and becomes chiral, although the molecules contain no chiral carbons. Recently, ferroelectric liquid crystal phases formed from achiral molecules have been reported in which smectic phases of banana-shaped molecules could show ferroelectric switching.<sup>8,9</sup> The existence of such a mesophase depends upon the length of the rigid core and the number of carbon atom in linear side wings as well as the magnitude of bent and its position. Since the bent-core molecules are closely packed and are all aligned in the direction of bending, they form a unique smectic phase.<sup>10</sup>

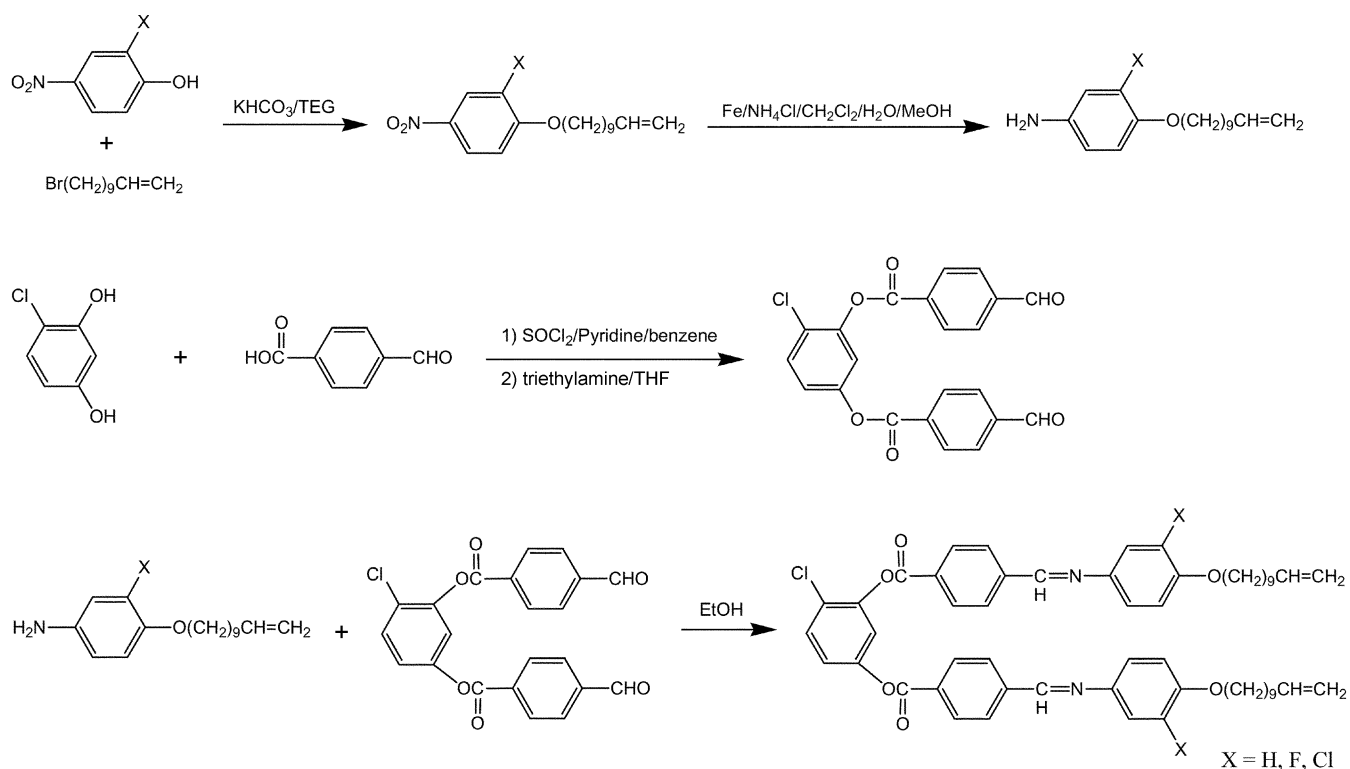
Niori *et al.*<sup>11</sup> reported the first obvious example of ferroelectricity in banana-shaped achiral molecules, ascribing the polar packing of the molecules with  $C_{2V}$  symmetry. Link *et al.*<sup>7</sup> reported the first spontaneous formation of chirality in a smectic phase of banana-shaped achiral molecules, a chiral layer structure with a handedness depending on the tilted molecular direction. Weissflog *et al.*<sup>12</sup> reported that ferroelectricity could be detected for one of the mesophases in some achiral banana-shaped molecules by varying direction of connecting groups and substituents. Currently, ferroelectric liquid crystals that exhibit spontaneous polarization due to their self-organizing character are regarded as one of the most promising groups of optoelectronic materials.<sup>5</sup>

In this study, new banana-shaped achiral molecules having vinyl end groups were synthesized, and their antiferroelectric liquid crystalline properties were investigated to determine the relationship between the liquid crystallinity and the structure of the vinyl groups. In our previous work, we obtained ferroelectric phase by controlling the number of

carbon atom in alkenyloxy chain<sup>13</sup> and introducing a polar lateral substituent in the 3-position of Schiff's base moiety of a bent-core molecule.

### Experimental Section

The syntheses of the banana-shaped molecules were performed according to a modified literature procedure,<sup>14,15</sup> and it is shown in Scheme 1. Since the synthetic procedures for 4-chloro-1,3-phenylene bis[4-{4-(10-undecenyloxy)phenyliminomethyl}benzoate] (C-PBUEB), 4-chloro-1,3-phenylene bis[4-{3-fluoro-4-(10-undecenyloxy)-(C-PBFUEB), and {3-chloro-4-(10-undecenyloxy)-(C-PBCUEB)-phenyliminomethyl}benzoate] were essentially same, we show only the one representative synthesis for C-PBUEB. First, 4-(10-undecenyloxy) aniline (I) was obtained by substitution reaction of 4-nitrophenol and 11-bromo-1-undecene. Then, 4-(10-undecenyloxy) aniline (I) was obtained by hydrogenation of 4-nitro-1-(10-undecenyloxy)benzene with iron in the presence of  $\text{CH}_2\text{Cl}_2/\text{MeOH}/\text{H}_2\text{O}$  solvent mixture. Next, 4-chloro-1,3-phenylene bis (4-formyl benzoate) (II) was prepared by reaction of 4-chloro-resorcinol and 4-formyl benzoyl chloride in tetrahydrofuran with triethylamine at 0 °C. Finally, the product was prepared by condensation reaction between the aniline (I) and the dialdehyde (II). The final product was purified by chromatography on silica gel, and recrystallized several times from a mixture of ethanol and dimethylformamide (20 : 1, v/v). Yield after purification was 20-30%. The representative spectroscopic data are as follows:  $^1\text{H NMR}$  ( $\text{CDCl}_3$ ) for C-PBUEB;  $\delta$  in ppm = 1.1-



Scheme 1

1.5 [m, 24H,  $-(\text{CH}_2)_6-$ ], 1.9 (m, 4H,  $-\text{OCH}_2\text{CH}_2-$ ), 2.0 (m, 4H,  $-\text{CH}_2\text{CH}=\text{}$ ), 4.0 (t, 4H,  $-\text{OCH}_2-$ ), 5.0 (q, 4H,  $=\text{CH}_2$ ), 5.8 (m, 2H,  $-\text{CH}=\text{}$ ), 6.9-8.3 (m, 19 H, Ar-H), 8.5 (s, 2H,  $-\text{CH}=\text{N}-$ ); EIMS  $m/z$  894(M). HRMS (EI) calcd for  $\text{C}_{56}\text{H}_{63}\text{ClN}_2\text{O}_6$  ( $\text{M}^+$ ): 894.4375. Found: 894.4362. The other banana-shaped compounds were also prepared and confirmed by the same method with C-PBUEB.

NMR spectra were obtained by Bruker DRX NMR spectrometer (500 MHz). Mass spectra were measured on a JEOL JMS-700 spectrometer. The transition behaviors were characterized by differential scanning calorimetry (Perkin-Elmer DSC7) and a polarizing microscopy (Nikon Eclipse E400 POL). DSC measurements were performed in  $\text{N}_2$  atmosphere with heating and cooling rate of  $5^\circ\text{C}/\text{min}$ . Optical texture observation was carried out using a polarizing microscope with a hot plate. The switching current was examined by the triangular wave method.<sup>16</sup> The sample cell was mounted in a microfurnace for measuring the spontaneous polarization with varying temperature. The temperature fluctuations inherent to the furnace were approximately  $0.1^\circ\text{C}$ . For direct measurement of the polarization, we used the triangular wave method for ease of subtracting the background current. The polarization current, converted into voltage signal through an amplifier, was measured in a digitizing oscilloscope and fed into a computer for data analyses.

SAXS measurements were performed in transmission mode with synchrotron radiation at the beamline 4Cl. Two-dimensional scattering patterns were collected on a CCD (charge coupled device) detector (Roper Scientific) with a wavelength of  $1.608 \text{ \AA}$ . The observed intensity was corrected for background scatter and absorption by the sample. Since the samples exhibited typical isotropic scattering patterns in the absence of an external field, the intensity data were normalized to one-dimensional scattering patterns by integration through circular averaging to improve the data resolution, and therefore to reduce the measurement time. WAXS measurements were conducted with an apparatus consisting of an 18 kW rotating anode X-ray generator (Rigaku Co.) operated at  $50 \text{ kV} \times 20 \text{ mA}$ , mirror optics with point focusing, and a one-dimensional position sensitive detector (M. Braun Co.). The  $\text{CuK}\alpha$  radiation ( $\lambda = 1.542 \text{ \AA}$ ) from a  $0.1 \times 1 \text{ mm}^2$  microfocus cathode was used. A beam path was maintained under vacuum to reduce air scattering, and tungsten foil ( $50 \text{ }\mu\text{m}$ ) was used for primary beam protection. The data are presented as a function of  $q = 4\pi\sin(2\theta)/\lambda$ , where  $2\theta$  is the scattering angle and  $\lambda$  is the X-ray wavelength. In order to investigate structural changes on heating and cooling, the samples were held in an aluminum sample holder, sealed with a window of  $7 \text{ }\mu\text{m}$  thick Kapton film on both sides. The sample was heated with two

cartridge heaters and its temperature was monitored by a thermocouple placed close to the sample.

## Results and Discussion

**Synthesis and mesogenic behaviors.** The synthetic route for the banana-shaped compound is rather straight forward and each reaction step is relatively well-known. The obtained compounds were characterized by means of NMR and Mass spectroscopy. NMR and Mass spectral data were in accordance with expected formulae. The phase transition temperatures depending on lateral halogen-substituents in the Schiff's base moiety are shown in Table 1. The introduction of a lateral polar substituent in the 3-position of Schiff's base moiety results in a decrease of the melting temperature over nonpolar substituent compound. This is because the presence of a polar lateral substituent prevents the regular stacking of molecules. The introduction of a polar group into the 3-position of the Schiff's base moiety could also affect the mesophase formation in two ways depending on polarity. First, it is expected that an electron-donating group could enhance electrostatic repulsion in the direction of the dipoles. Secondly, an electron-withdrawing group could decrease electrostatic repulsion in the direction of the dipoles. Thus, the banana-shaped molecules with a polar substituent can form the switchable smectic phases. As shown in Table 1, among the compounds synthesized, the smectic phase having a lateral fluorine substituent at 3-position of the Schiff's base moiety showed only switching property.

**Microscopic textures.** Using an optical microscope with crossed polarizer, we could identify every phase transitions on cooling the isotropic as shown in Table 1. As shown in Figure 1(a), when the isotropic liquid of C-PBFUEB with  $\text{X}=\text{F}$  is cooled slowly, optical texture of the smectic phase appears as a germ-like structure. The texture tends to transform into aggregative germ domain shown in Figure 1(b), and then the smectic phase is changed abruptly to paramorphic texture shown in Figure 1(c). Finally, the texture grows to become colorful mosaic texture with schlieren remnants to room temperature as shown in Figure 1(d).

**Switching current and spontaneous polarization.** In order to characterize the smectic phase, we measured the spontaneous polarization of the sample. For the measurement, a cell is made up of conductive indium-tin-oxide coated glasses, treated with rubbed polyimide for the alignment. The cell gap was maintained by patterned organic spacer of  $1.5 \text{ }\mu\text{m}$  thickness. The spontaneous polarization was measured by applying triangular shape voltage, and the

**Table 1.** Phase transition temperatures on cooling and switching property depending on a lateral halogen-substituent

Sample code	Transition Temperature/ $^\circ\text{C}$ (Enthalpy/ $\text{J mol}^{-1}$ )	Switching Property
X = H	Cr 78.1 (14.9) SmX <sub>1</sub> 121.6 (11.2) I	None
X = F	Cr 36.3 (11.2) SmX <sub>1</sub> 110.2 (6.7) SmX <sub>2</sub> 111.8(6.4) I	Switchable
X = Cl	Cr 82.1 (2.9.) SmX <sub>1</sub> 92.8 (3.4) I	None

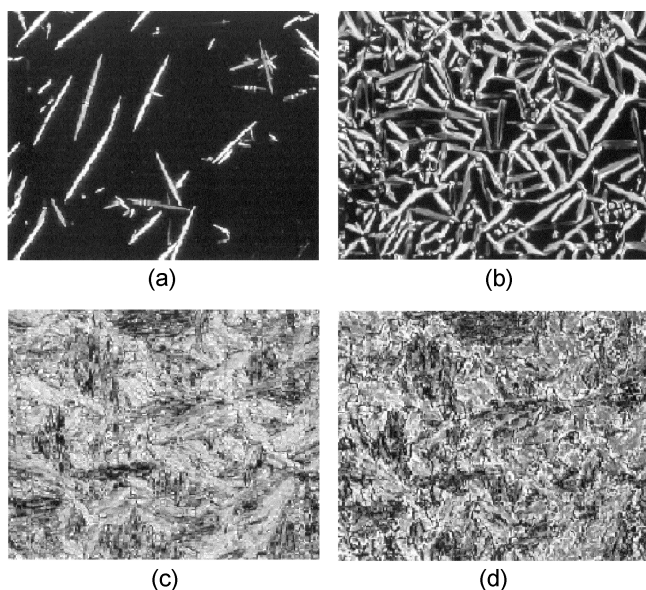


**Figure 1.** Optical micrographs of Sm C\* phase for C-PBFUEB with X=F on cooling from the isotropic liquid: (a) The phase appears as germ-like structure; (b) The texture tends to transform into aggregative germ-domain; (c) As it was further cooled, the smectic phase is changed abruptly to paramorphic texture at 105 °C; (d) Then, the texture grows to become colorful mosaic-texture with schlieren remnants to room temperature.

switching was also observed by using a polarized microscope. Figure 2 shows the polarization reversal current for C-PBFUEB with X=F at the temperature corresponding to the smectic phase, SmX<sub>1</sub>. In Figure 2, the two peaks of reversal current for every half period were observed at 106 °C, 86 °C, and 60 °C (temperature within the smectic phase forming region), respectively. Thus, we can conclude that the smectic phase of the compound (C-PBFUEB) is antiferroelectric with the tip of the bent molecule orienting along the electric field and reversing its orientation on the polarity of the field. Figure 3 shows temperature dependence of spontaneous polarization for C-PBFUEB in the cooling experiment. In Figure 3, a switchable smectic phase exhibits a maximum polarization of about 250 nC/cm<sup>2</sup>. On cooling the isotropic liquid, the spontaneous polarizations are increased with decreasing temperature. The spontaneous polarization was increased dramatically with lowering temperature until a critical temperature. The sharp increase of polarization suggested that the isotropic phase-to-smectic phase transition is the first order. On further lowering the

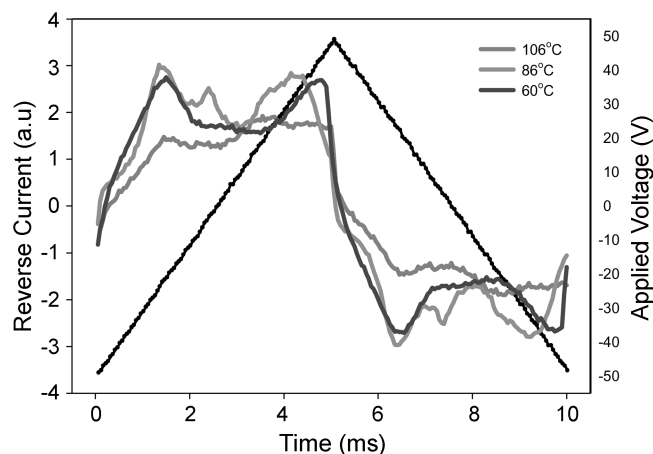


**Figure 2.** The switching current curves obtained by applying a triangular voltage wave for C-PBFUEB at 60 °C, 86 °C, and 106 °C.

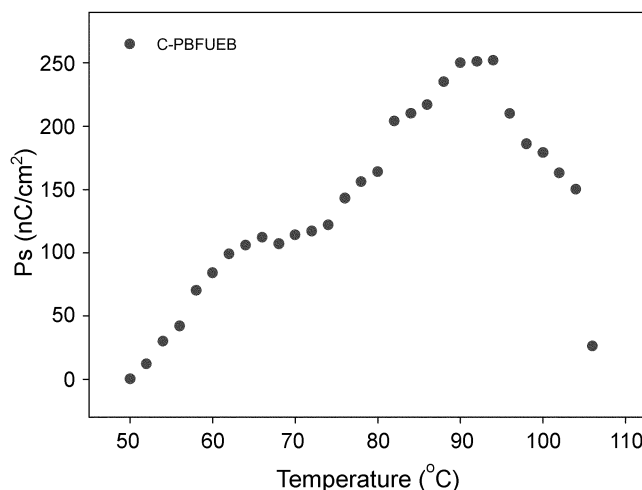


**Figure 3.** The temperature dependence of spontaneous polarization for C-PBFUEB.

temperature under 36 °C, the polarization was vanished, because of crystallization of the central rod parts of the molecules. Figure 4 shows the textural changes of the switching states on applying different electric fields. When C-PBFUEB sample is filled in the cell, virgin domains, which are formed spontaneously on cooling the isotropic phase, are sensitive to the sign of the electric field. Applying an electric field of 5 V/μm<sup>-1</sup> to the electro-optical cell, birefringence color on the virgin domain with a blue mixed

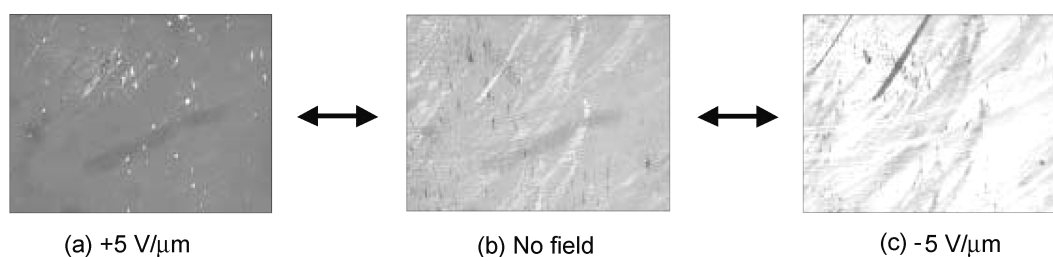


**Figure 4.** Textural change of the switched states of a C-PBFUEB cell under different electric fields. The domains formed after cooling the clear isotropic phase: (a)  $E = +5$ , (b)  $E = 0$ , (c)  $E = -5$  V/μm<sup>-1</sup>.

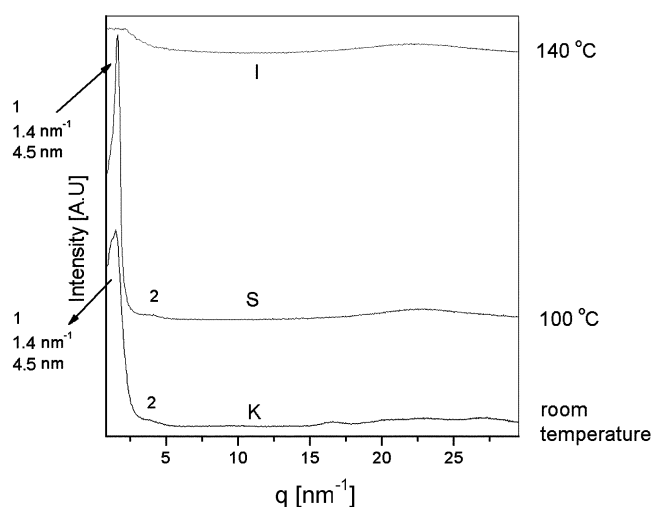


**Figure 5.** Temperature dependence of the small and wide angle X-ray diffraction patterns of C-PBFUEB with X=F.

with purple is formed. But, applying an electric field of  $-5 \text{ V}\mu\text{m}^{-1}$  field, birefringence color of the domain is changed to the striped yellow mixed with blue. According to Link *et al.*,<sup>7</sup> there are regions within an electro-optical cell where the textural domain of the switched state differs with opposing sign of the applied electric field. The occurrence of such regions depends on the history of the sample but also on the material.

**X-ray study.** Figure 5 displays the X-ray diffraction (XRD) patterns at given temperature. In Figure 5, the XRD pattern of C-PBFUEB with X=F at room temperature shows several diffraction peaks (denoted as K), indicating the presence of a crystalline structure. As sample was heated to 100 °C (above the transition temperature of 36.3 °C by

DSC), the smectic characteristics (denoted as S) of a broad wide-angle peak and a narrow small angle-peak were obtained. Since no crystalline peaks are found in wide angle region, this XRD pattern is indicative of a smectic phase having a layer spacing with a 1 : 2 ratio of peak scattering vectors. The lattice spacing of a smectic phase was calculated to be  $4.5 \text{ nm}^{-1}$  from the relative sharp peak at  $q = 1.4 \text{ nm}^{-1}$ . In the isotropic phase (above the transition temperature of 111.7 °C by DSC), the small angle peak (denoted as I) was disappeared as shown in Figure 5. Figure 6(a) shows small angle XRD patterns of C-PBFUEB at different temperatures. Figure 6(b) shows the wide angle XRD patterns of C-PBFUEB. On heating to 100 °C (above the transition temperature of 36.3 °C by DSC), an amorphous hollow appears in the wide angle region. This XRD pattern is indicative of a smectic phase having a layer spacing with a 1 : 2 ratio of peak scattering vectors.

## Conclusions

The introduction of a polar lateral substituent in the 3-position of a Schiff's base moiety reduced the transition temperature and the degree of crystallinity of the switchable banana liquid crystal. The presence of vinyl groups onto the terminals of a bent-core molecule reduced the melting and clearing temperature. The bent-core molecule with undecyloxy group onto the terminal chain could form the switchable smectic phase even though the constituent molecules are achiral. We could obtain antiferroelectric phase by introducing a fluorine substituent in the 3-position of Schiff's base moiety of banana-shaped molecule. By analyzing the XRD patterns, we could also find that a smectic phase of C-PBFUEB has a layer spacing of  $4.5 \text{ nm}^{-1}$  with 1 : 2 ratio of peak scattering vectors.

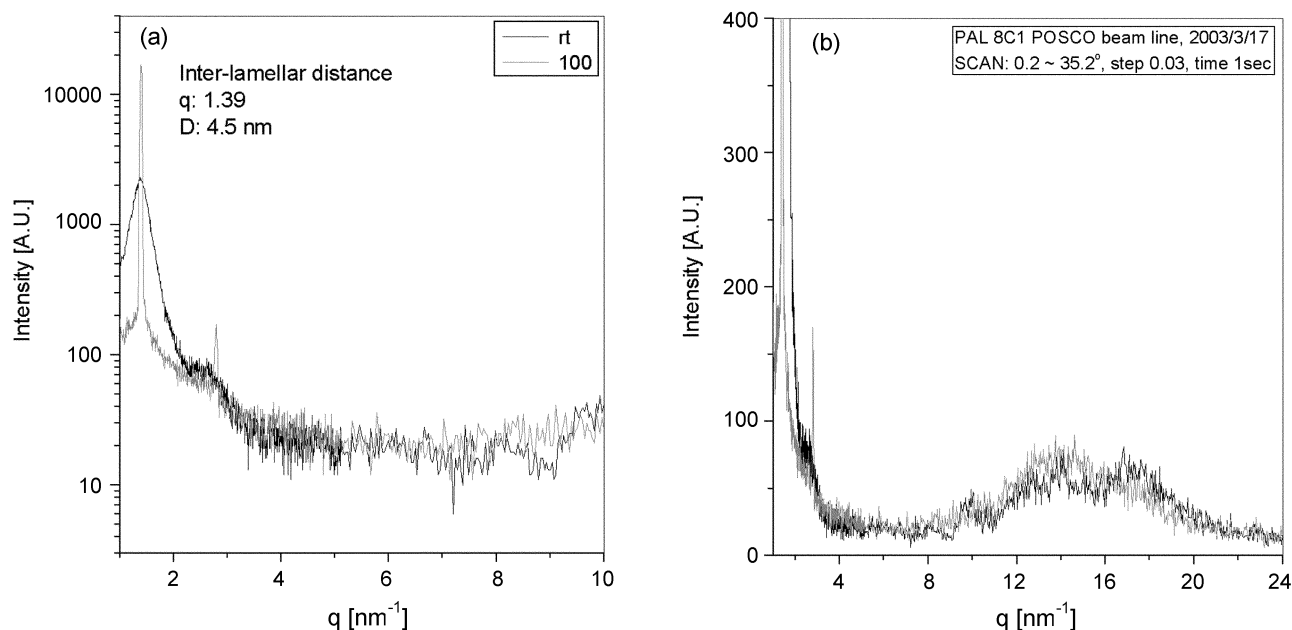


**Figure 6.** (a) Small angle diffraction patterns and (b) wide angle diffraction patterns of C-PBFUEB with X=F at different temperatures.

**Acknowledgement.** This work was supported by grant No. R01-2001-00433 from the Korea Science & Engineering Foundation and the GSNU Chemistry Research Fund.

### References

1. Kondepudi, D.; Kauffmann, R. J.; Singh, N. *Science* **1990**, 250, 975.
  2. Qiu, X.; Ruiz-Gracia, J.; Stine, K. J.; Knobler, C. M.; Selinger, J. *Phys. Rev. Lett.* **1991**, 67, 703.
  3. Lennan, M.; Seul, M. *Phys. Rev. Lett.* **1992**, 69, 2082.
  4. Pang, J.; Clark, N. A. *Phys. Rev. Lett.* **1994**, 73, 2332.
  5. Walba, D. M.; Dyer, D. J.; Sierra, T.; Cobben, P. L.; Shao, R.; Clark, N. A. *J. Am. Chem. Soc.* **1999**, 118, 1211.
  6. Walba, D. M. *Science* **1995**, 270, 250.
  7. Link, D. R.; Natale, G.; Shao, R.; MacLennan, J. E.; Clark, N. A.; Korblova, E.; Walba, D. M. *Science* **1997**, 278, 1924.
  8. Tournihac, F.; Blinov, L. M.; Simon, J.; Yablonsky, S. V. *Nature* **1992**, 359, 621.
  9. Sekine, T.; Takanishi, Y.; Niori, T.; Watanabe, J.; Takezoe, H. *Jpn. J. Appl. Phys.* **1997**, 36, L1201.
  10. Lee, C. K.; Chien, L. C. *Ferroelectrics* **2000**, 243, 231.
  11. Niori, T.; Sekine, T.; Takezoe, H. *J. Mater. Chem.* **1996**, 6, 1231.
  12. Weissflog, W.; Lischka, Ch.; Benne, I.; Schare, T.; Pelzl, G.; Diele, S.; Kruth, H. In *Proceedings of the European Conference on Liquid Crystals, Science and Technology*; Zaopane, Poland, March 3-8, 1997; pp 126-132.
  13. Kwon, S. S.; Kim, S. T.; Lee, C. K.; Shin, S. T.; Oh, L. T.; Choi, E. J.; Kim, S. Y.; Chien, L. C. *Bull. Korean Chem. Soc.* **2003**, 24(3), 274.
  14. Hassen, A.; Alexanian, V. *Tetrahedron Lett.* **1978**, 447.
  15. Lee, C. K.; Kwon, S. S.; Shin, S. T.; Choi, E. J.; Lee, S. N.; Chien, L. C. *Liq. Cryst.* **2002**, 29(8), 1007.
  16. Miyasato, K.; Abe, H.; Takezoe, A.; Kuze, E. *Jpn. Phys.* **1983**, 22, L661.
-